Available online at www.sciencedirect.com
ScienceDirect
Journal of the European Ceramic Society 29 (2009) 637–646
www.elsevier.com/locate/jeurceramsoc

A model of growth of titanium dioxide crystals with simultaneous transformation from anatase to rutile

Ian L. Cooper, Terry A. Egerton *, Fulian Qiu

School of Chemical Engineering and Advanced Materials, Bedson Building, Newcastle University, Newcastle on Tyne NE1 7RU, UK

Received 20 May 2008; received in revised form 21 July 2008; accepted 24 July 2008
Available online 11 September 2008

Abstract

This study simulates the combination of crystal growth by evaporation–condensation with the potential for a phase change once the crystals have reached a critical size.

Crystal growth has been simulated as a two-dimensional Monte Carlo process in which the probability of accepting or rejecting an individual evaporation–condensation step is given by the Metropolis algorithm. Crystals, taken to be of the anatase form of TiO_2, which have grown larger than a specified critical size may transform irreversibly to a second phase, taken to be rutile. The probability of conversion increases with increasing crystal size. For each critical size there exists a limited range over which the transformation kinetics follow the familiar relationship $\alpha = 1 - \exp(-kt^n)$ (where α is the fractional conversion at time, t). The dependence of the mean size of the two polymorphs and of the rutile size-spread (rms) on critical size have been investigated. The most significant aspect of the plots of the normalized size-spread, rms/mean-size, is its gradual increase as the rutile fraction increases from 0.75 to 0.98.

Keywords: Grain growth; Calcination; Optical properties; TiO_2; Monte Carlo modelling

1. Introduction

Titanium dioxide is usually found, and is manufactured commercially, as one of the two polymorphs—anatase and rutile.[1,2] Although large crystals of rutile are thermodynamically more stable than those of anatase at all temperatures[3] both low temperature precipitation processes and high temperature gas phase oxidation reactions typically give TiO_2 with a very high anatase content unless special steps are taken to yield rutile. Thus, in the gas phase production of TiO_2, $AlCl_3$ is added in order to convert the predominantly anatase product into the rutile form.[1,2] Alternatively, in the 'sulphate process' production of TiO_2 pigment, the precipitation of titanium dioxide from sulphuric acid solutions results exclusively in formation of anatase which is usually nanocrystalline with a crystallite size of ~10 nm.[2] When the fine precipitate is heated, the anatase crystals grow and in addition are converted to rutile. The mean size of the rutile crystals is normally larger than that of the anatase from which they are formed.[4]

The surface free energy of rutile exceeds that of anatase; i.e., the surface enthalpy of rutile is estimated to be 1.8 J m^{-2} greater than that of anatase[5] although the $T\Delta S$ terms are considered to be broadly equivalent for the two forms.[5–7] Consequently, for small particles, the surface contribution is sufficiently large to make the total of the surface and bulk energies of anatase less than the sum of the surface and bulk energies of rutile. According to this argument anatase–rutile transformation occurs when an anatase crystal grows to a size at which the surface contribution to its energy is no longer sufficient to compensate for the lower energy of massive rutile crystals. Banfield and Zhang[8] suggested that anatase is more stable than rutile if the particle size is below ca. 14 nm. The approach has been generalized to the transformation of amorphous TiO_2 to anatase[9] and to include the effect of water on the crystal morphology and hence the critical size of the anatase to rutile transformation.[10] The kinetics of the anatase to rutile transformation have been followed by using powder X-ray diffraction (X-ray line broadening)[11,12] to monitor

* Corresponding author. Tel.: +44 191 222 5618.
E-mail addresses: Ian.Cooper@ncl.ac.uk (I.L. Cooper), T.A.Egerton@ncl.ac.uk (T.A. Egerton).

0955-2219/$ – see front matter © 2008 Elsevier Ltd. All rights reserved.
doi:10.1016/j.jeurceramsoc.2008.07.059

the transformation, and the mean-size of both the anatase and rutile crystals during either an isothermal or temperature programmed calcination process. A large number of experimental studies has focused on the sensitivity of the transformation and the crystal growth processes to the presence of inorganic additives.[13,14] However, attempts to interpret the results in terms of simple kinetic models have been less successful. Thus a recent survey[15] reported that standard 1st order, standard 2nd order, contracting spherical interface and nucleation and growth of overlapping nuclei models all fail to satisfactorily represent the measurements. Similarly, Zhang and Banfield[16] interpreted the dependence of the measured activation energy of nucleation on both particle size and packing as a consequence of the change in the locus of the predominant nucleation from interface to surface to bulk. The same authors also reported[17], that the well-known relationship[16]

$$\alpha = 1 - \exp(-kt^n) \tag{1}$$

where α is the fractional conversion at time t, and k and n are constants, did not hold for the transformation of amorphous titania to anatase.

In a previous paper[18] we used the Ising model[19] to explore particle growth and associated particle size distributions within an evaporation (or dissolution)–condensation model of particle growth. A key feature of the model is that, because the energy of a surface with high curvature exceeds the energy of low-curvature surfaces, large particles grow at the expense of small ones. The same principle, though expressed via the Gibbs-Thomson equation, is employed by Madras and McCoy[20,21] in their treatments of Ostwald ripening through successive evaporation (or dissolution) and condensation steps. A significant feature of their treatment, based on population balance equations for the size distribution of the dimorphs, is the evaluation of the particle polydispersity index with time. Although there were significant challenges associated with our previous approach – particularly in the choice of the model parameters – its use enabled the influence of key experimental parameters on the crystal size distribution (a property of great import with respect to the use of TiO_2 as both a pigment and as a ceramic raw material) to be explored in a full and systematic manner. In this present paper, we extend the earlier model to explore the particle sizes and particle size distributions which arise from the growth of anatase particles to specifically include the possibility of their transformation from anatase to rutile. In order to do this, we have introduced the additional assumption that once the evaporation–condensation process leads to particles which exceed a critical size, the anatase form has the opportunity to convert irreversibly to the rutile form of titanium dioxide.

2. Simulation procedure

Our simulation domain is two-dimensional, discretized as a 400×400 square lattice with a specified fractional occupancy, as described previously.[18] Filled and empty sites are assigned spin orientations of +1 and −1, respectively, and a set of adjacent filled sites form a crystal surrounded by empty space. The driving force for growth is the reduction in surface energy, which takes the form.

$$E = \frac{1}{2}{\sum_{ij}}' J_{ij}\omega_{ij} \tag{2}$$

where $J_{ij} = J$ when i and j have spin orientations of opposite sign, and $J_{ij} = 0$ otherwise. The prime on the summation indicates that $i \neq j$ and the factor of 1/2 eliminates double counting. The term ω_{ij} refers to first, ω_f, and second, ω_s, nearest neighbour weightings. Specifically, $\omega_{ij} = \omega_f = 1$ when lattice sites i and j share a common side, $\omega_{ij} = \omega_s$, $(0 < \omega_s < 1)$, when they share a common corner and $\omega_{ij} = 0$ otherwise. The ratio ω_s/ω_f is referred to as 'the nearest neighbour weighting'.

The microstructure evolves as a result of transport and crystal transformation. A spin is transported from one boundary site to another, with opposite spin orientation, to represent an evaporation–condensation process. The energy difference ΔE associated with the two relevant configurations is calculated and the probability $p(\Delta E)$ of accepting or rejecting such an evaporation–condensation step is given by the Metropolis algorithm[18], whereby

$$p(\Delta E) = 1 \quad \text{when } \Delta E \leq 0 \tag{3}$$

and

$$p(\Delta E) = \exp\left(\frac{-\Delta E}{k_B T}\right) \quad \text{when } \Delta E > 0 \tag{4}$$

Hence for negative (or zero) ΔE the step is allowed, whereas for positive ΔE the step is allowed only if the exponential term is greater than a random number between 0 and 1. Here, T denotes the absolute temperature and k_B the Boltzmann factor. The interaction energy will be expressed via the dimensionless temperature parameter $k_B T/J$.

The mechanism of crystal transformation is based on the notion of a critical size for an anatase crystal and the transformation procedure is invoked following accepted condensation processes.

It will be appropriate to assume that the evaporated pixel is neither anatase nor rutile; it will be referred to as a titania pixel. We adopt the criterion that condensation on to anatase of a titania pixel generated by evaporation results in a probability of conversion of the resultant anatase to rutile only when the size, S, exceeds a critical value, S_L, with probability of transformation given by

$$P_T = \left(\frac{S - S_L}{S}\right)^m \tag{5}$$

where m is an integer. Specifically, using A_n and R_n to denote anatase and rutile crystals, respectively, of size n, we have

$$T + A_n \rightarrow A_{n+1} \quad \text{when } n < L \tag{6}$$

$$T + A_n \rightarrow A_{n+1} \quad \text{when } n \geq L \text{ and } P_T \leq r \tag{7}$$

$$T + A_n \rightarrow R_{n+1} \quad \text{when } n \geq L \text{ and } P_T > r \tag{8}$$

and

$$T + R_n \rightarrow R_{n+1} \quad \text{for all } n \tag{9}$$

where T denotes a titania pixel and r denotes a random number between 0 and 1. When an anatase pixel is converted to a rutile pixel, its spin orientation of +1 is replaced by +2. No energetic implications are invoked; the '+2' serves only as a distinguishing label for counting purposes. In contrast to the treatment of Madras and McCoy[20,21] in which clusters smaller than the critical nucleus are deemed unstable and instantaneously disappear the rutile phase is retained in all evaporations from rutile and in all energetically accepted condensations on to rutile.

3. Results and discussion

The effects of a range of parameters on growth were first examined. Fig. 1 shows 'snapshots' of the growth during a simulation for an initially random distribution of grains with a lattice occupancy of 25%. (These snapshots are typical images selected from one of the five replicate runs from which numerical characterization is normally based.) Any crystals of size greater than S_L which arise from the initial random distribution may be coded as rutile on a random basis. The filled cells represent crystals, with the dark cells (blue cells, in online version) representing anatase and the light cells (red cells in online version) representing rutile—the phase which only becomes stable once a critical crystal size has been exceeded. Time in the simulation is measured in units of Monte Carlo steps (MCS) where one MCS corresponds to a number of attempted exchanges equivalent to the total number of lattice sites, in this case 16×10^4. As the number of MCS increases some crystals grow at the expense of others and this growth is determined by both the value of k_BT/J (=1.0 for this example) and the value of ω_s/ω_f (=0.5 in this case). As the crystals grow, the initial anatase crystals may convert to rutile; the conversion is controlled by the choice of critical size, and by the value of the integer m in Eq. (5). In the simulation, shown in Fig. 1, the critical size, S_L, was selected as 100 (with $m = 3$). To put this choice of critical size in context, an individual pixel may be envisaged as equivalent to one

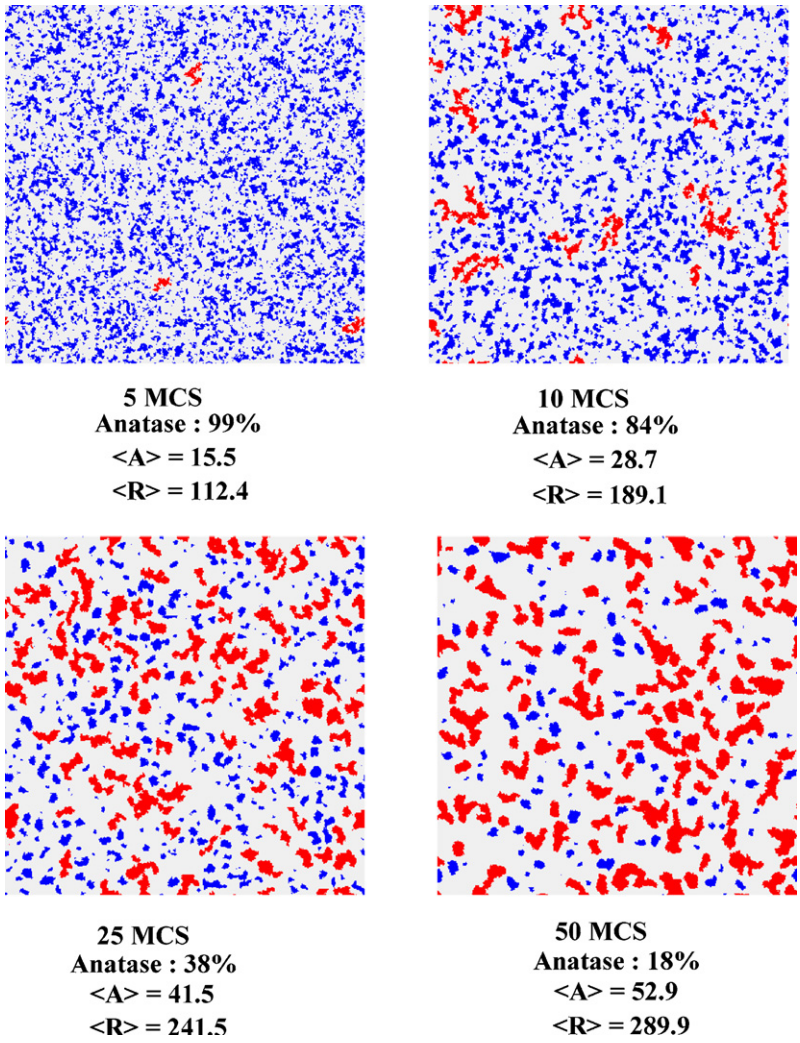

Fig. 1. Snapshots, from an initially random distribution, at various Monte Carlo Steps (MCS). Light (blue in the electronic version) corresponds to anatase, dark (red in the electronic version) to rutile. The matrix size is 400 × 400, the fractional occupancy is 25% and the value of the temperature parameter (k_BT/J) is 1.0. The nearest neighbour weighting (ω_s/ω_f) is 0.5 and transformation from anatase to rutile is permitted once the cluster size exceeds 100. Quoted are the anatase fraction, and the mean sizes of anatase ($\langle A \rangle$) and rutile ($\langle R \rangle$). (For interpretation of the references to colour in this figure legend, the reader is referred to the web version of the article.)

Table 1
The values, at 25 MCS, of percentage rutile, %R, anatase mean size, ⟨A⟩, and rutile mean size, ⟨R⟩, from 10 separate runs compared with the average of all 10 results and with the averages based on two sub-sets of 5 runs

						Average of 5 runs	Average of 10 runs
%R Run 1–5	62	63	62	64	58	62	
%R Run 6–10	59	65	59	58	63	61	61
⟨A⟩ Run 1–5	43.2	41.3	44.1	38.9	43.4	42.2	
⟨A⟩ Run 6–10	42.4	39.8	42.5	44.5	44.6	42.8	42.5
⟨R⟩ Run 1–5	213.2	239.5	240.1	216.7	235.6	229.0	
⟨R⟩ Run 6–10	231.4	246.8	211.6	231.1	225.6	229.1	229.1

Parameter values as in Fig. 1.

tetragonal unit cell (lattice parameters a and c) of anatase. The notional surface area of this pixel, estimated as $1/3(2ac + c^2)$, is 0.54 nm^2. A critically sized two-dimensional crystal consisting of 100 pixels ($S_L = 100$) would then have a notional 'diameter' of ~8.5 nm, which is comparable with the critical size of 14 nm suggested by Banfield and Zhang.[8]

Overall the simulated growth sequence shows clearly the conversion of small anatase crystals to larger rutile crystals. After 50 MCS, the anatase mean size has increased from an initial value of 2 to a value of 53. The rutile percentage has grown from 0 to 82 and the rutile mean crystal size has reached 290. As anatase grows the larger crystals are increasingly likely to transform to rutile, causing the mean size of rutile to be greater than that of anatase.

The above comments are based on 'snapshots' of individual runs at a lattice occupancy of 25%. Table 1, also for a lattice occupancy of 25%, compares values (of % rutile, mean anatase size, ⟨A⟩, and mean rutile size, ⟨R⟩) after 25 MCS estimated in a series of 10 such runs with those obtained by averaging the same results, into two sub-sets of 5 and one set of 10. It demonstrates the improved repeatability associated with taking the average of five runs, and the negligible further gain on taking the average of 10 runs. Consequently, the results in the rest of this paper are averages from five separate runs.

3.1. Effect of critical size

A significant parameter in our model which influences the anatase to rutile transformation is the critical size, S_L; of anatase crystals above which conversion from anatase to rutile becomes possible. Although the probability, P_T, of transformation (Eq. (5)) includes a variable integer exponent, m, this will be held fixed at a value of 3, as will be discussed below. Fig. 2 shows the variation of the fraction of rutile (equivalent to one minus the fraction of anatase) with the number of Monte Carlo Steps (MCS) for values of critical size varying from 20 to 150. The remaining parameters are held constant, with values $\omega_s/\omega_f = 0.5$, $k_B T/J = 1.0$, $m = 3$ and lattice occupancy of 25%. For clarity, only the first 50 MCS are shown in Fig. 2, although the simulations were run for 200 MCS. As S_L increases, an increase in induction time for rutile formation and a decrease in overall rate of conversion from anatase to rutile are apparent. This relates to the fact that as the critical size is increased, anatase particles must grow to a larger size before conversion to rutile becomes feasible. The (average) number of MCS required to achieve 90% conversion from anatase to rutile increases; specifically, 13, 27, 42, 60, 79, 87 and 126 MCS for values of critical size $S_L = 20, 40, 60, 80, 100, 120$ and 150, respectively. Although the induction step predicted by the present model is not obvious in the experimental results at 520 °C reported by Zhang and Banfield[22] in their Fig. 1a, it is much clearer in the pattern of results from 480 to 580 °C available in Fig. S1 of the supplementary information for that paper. At 480 °C an induction time for rutile formation was found for all anatase sizes from 8 to 20 nm. At 500 °C the induction period was more obvious for the smaller, 8–12 nm, particles, which would need to grow to above the critical size before transforming to rutile. It is the existence of this induction step which makes the standard analytical models surveyed by Madras, McCoy and Navrotsky[15] inapplicable.

Plots of the mean sizes of anatase, ⟨A⟩, and rutile, ⟨R⟩, against MCS are shown in Fig. 3a and b, respectively, for selected values of S_L, and show that an increase in the value of S_L leads to an increase in the mean size of *both* anatase and rutile. In the case of anatase, the initial increase in mean size with increasing value of S_L is a consequence of the greater opportunity for growth before further increase is curtailed through conversion to rutile at longer simulation times, when the mean anatase size falls because larger anatase crystals have converted to rutile. However, a plot of the mean size of anatase, ⟨A⟩, against rutile fraction, displayed in Fig. 3c, shows that when the rapid decrease in ⟨A⟩ occurs, few unconverted anatase crystals remain. We also note from Fig. 3c that the maximum mean size of anatase crystals is approximately 50% of the value of the critical size, S_L.

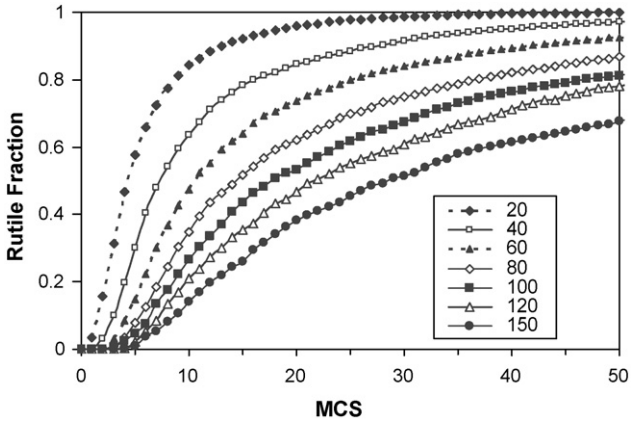

Fig. 2. Rutile fraction versus MCS, for selected values of critical size (S_L) between 20 and 150. In all cases, the occupancy is 25%, the nearest neighbour weighting is 0.5 and the temperature parameter is 1.0.

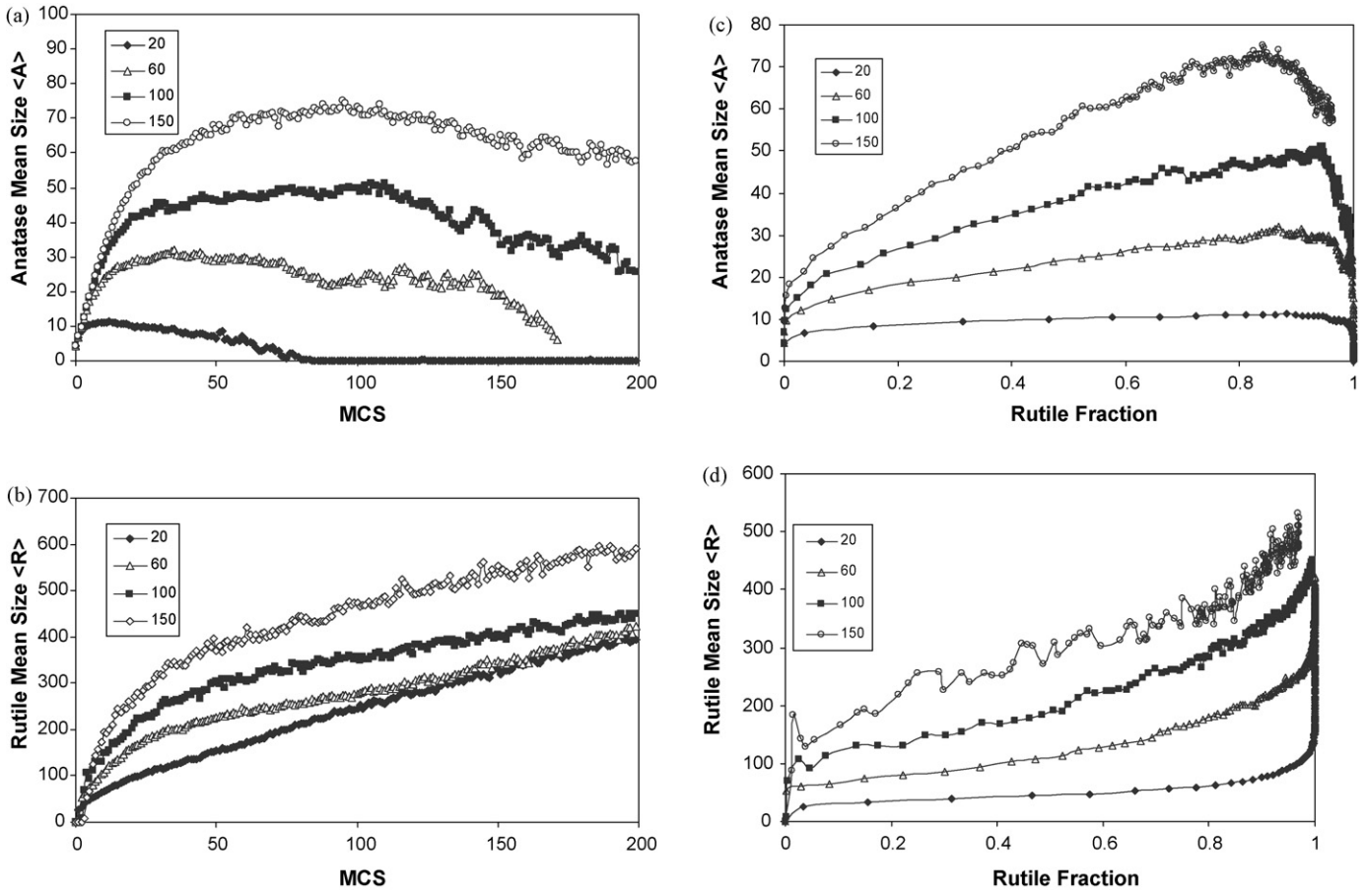

Fig. 3. For selected values of critical size (S_L), (a) anatase mean size (⟨A⟩) versus MCS. (b) Rutile mean size (⟨R⟩) versus MCS. (c) Anatase mean size (⟨A⟩) versus rutile fraction. (d) Rutile mean size (⟨R⟩) versus rutile fraction. In all cases, the occupancy is 25%, the nearest neighbour weighting is 0.5 and the temperature parameter is 1.0.

For rutile, Fig. 3b, a plot of mean size ⟨R⟩ versus MCS as a function of critical size, S_L, shows a short induction period, which increases with increasing value of S_L. Beyond this induction period, ⟨R⟩ increases with increasing value of S_L. Both these effects arise because there are no rutile crystals smaller than the value of S_L. At 50 MCS, the rutile mean size is seen to increase almost linearly from ∼140 to ∼370 as S_L increases from 20 to 150. A plot of ⟨R⟩ versus rutile fraction, Fig. 3d, shows very large changes in rutile mean size during the last stages of the conversion, and demonstrates why commercial production of sulphate-route titania pigments targets a rutile content of ∼98.5%. On average, a 3% change in percentage rutile from 92% to 95% causes an 8% increase in rutile mean size. However, a similar 3% change in percentage rutile from 95% to 98% causes a 12.5% increase in ⟨R⟩. The model suggests that any attempt to achieve a higher conversion to rutile would lead to an unacceptably large range of crystal size.

As noted above, a second parameter which influences the probability of transformation from anatase to rutile is the integer exponent, m, occurring in Eq. (5). Since the term $(1 - S_L/S)$ must be less than 1 (S must exceed S_L for the transformation to be possible), as the value of m is increased, the probability of transformation declines. For example, an increase in the value of m from 1 to 5 reduces the value of rutile fraction at 50 MCS from 0.90 to 0.73. Further increase in m leads to a rapid decrease in rutile fraction. By comparison, an increase in S_L from 40 to 150 reduces the value of rutile fraction at 50 MCs from 0.97 to 0.68. Since the overall effect of increasing the value of m is similar to that of increasing the value of S_L, we hold m fixed (at the intermediate value of 3) and concentrate on changes to the more physically significant parameter S_L.

3.2. Effect of the parameter k_BT/J

The consequences of varying k_BT/J are interesting. In our previous simulation of crystal growth without phase change, [17] the change in growth rate with k_BT/J was not monotonic. Below a critical value of ∼0.67 the mean particle size at fixed MCS was almost independent of k_BT/J but above this critical value it decreased markedly, by a factor of 1.5, as k_BT/J rose from 0.67 to 1.5. Despite the complications introduced by anatase to rutile transformation, both the anatase growth (Fig. 4a) and the rutile growth (Fig. 4b) show a similar pattern. Both these plots are for 50 MCS. (In the region 100–200 MCS (not shown) the anatase mean size decreases with increasing MCS as large anatase crystals convert to rutile.) When, as in the earlier study, mean sizes corresponding to a fixed time (i.e. a fixed number of MCS) were computed, it became apparent that although the spread of results within each set of five was acceptable for values of k_BT/J far from the discontinuity, the range was much greater at values

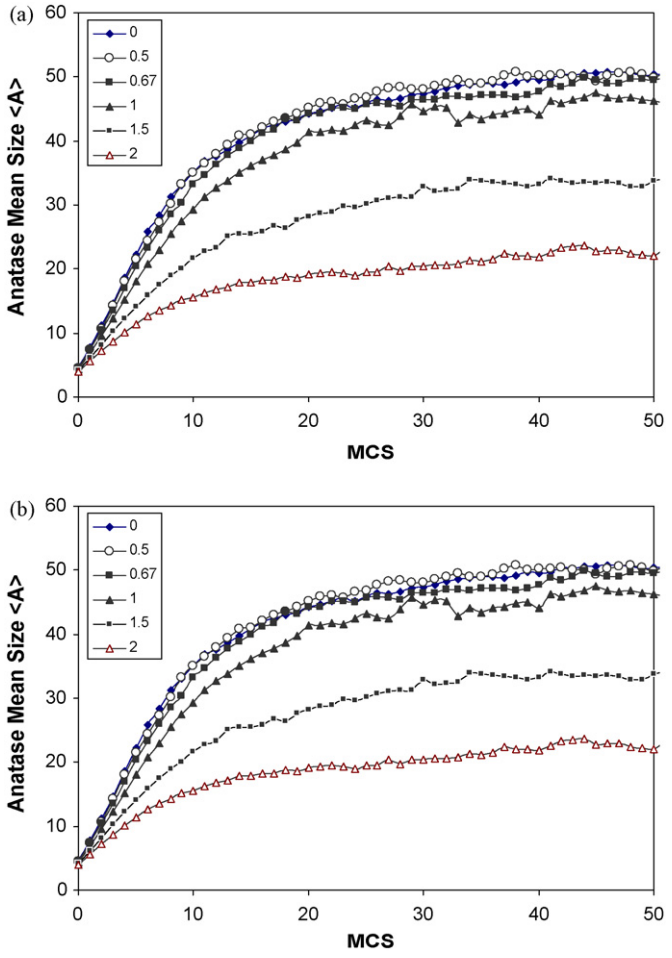

Fig. 4. For selected values of temperature parameter (k_BT/J), (a) anatase mean size (⟨A⟩) versus MCS. (b) Rutile mean size (⟨R⟩) versus MCS. In both cases, the occupancy is 25%, the nearest neighbour weighting is 0.5 and the critical size is 100.

near to it. When the average sizes for individual sets of 5 runs were plotted the mean anatase size decreased for $k_BT/J > \sim 0.65$, suggesting a critical temperature, even though it could not be identified precisely. The curve for rutile showed a maximum for $0.60 < k_BT/J < 0.80$ but, again, it was not possible to identify any discontinuity. A much clearer picture emerged when (Fig. 5) the results for constant composition, rather than constant simulation time, were considered. These results demonstrate clearly the cusp in the plot of rutile mean size versus k_BT/J. The critical temperature parameter k_BT_c/J corresponding to this cusp is ~0.67 and above this value both anatase and rutile mean sizes decrease. This decrease corresponds to the increased probability of accepting a positive energy change that is built into the model. Such positive energy moves correspond to pixel migration from particles of low curvature to particles of high curvature, i.e. from big to small particles and this leads to the observed decrease in mean size.

3.3. Effect of other parameters

In an earlier study,[18] in which growth was simulated without the possibility of transformation, the effects of lattice occupancy and the contribution of second nearest neighbours were systematically examined. In the present study, an increase in the occupancy of the 400×400 grid from 3% to 40% (for $\omega_s/\omega_f = 0.5$, $k_BT/J = 1.0$) led to more rapid rutilization. This is a consequence of the larger initial mean size at higher occupancies which means that fewer MCS are needed for the particles to grow to a size at which the anatase to rutile transformation becomes feasible. (The results for 3% occupancy are relatively scattered because of the small number of particles—only 48×10^2 pixels are occupied.) A general result was that, as for the results in Fig. 2d, the mean rutile size changed by less than a factor of 2 over the range 20–80% rutile but then increased greatly for rutile contents greater than 90%. We reported previously, in the absence of an anatase to rutile transformation, that the growth rate decreased as the weighting assigned to second nearest neighbor interactions decreased and, unsurprisingly, this behaviour was also found in this study for the initial stages of growth. The faster growth of anatase consequent upon a larger second nearest neighbour weighting leads to a faster transformation to rutile and to an earlier growth of the rutile crystals that are formed.

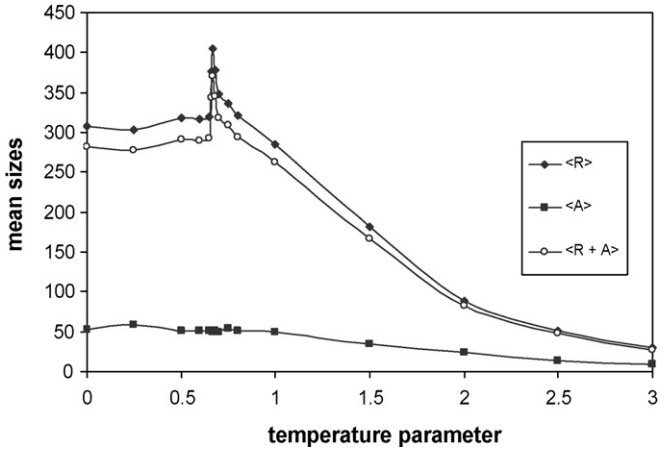

Fig. 5. Rutile (⟨R⟩), anatase (⟨A⟩) and overall (⟨R + A⟩) mean sizes versus temperature parameter k_BT/J corresponding to constant 90% conversion from anatase to rutile. The occupancy is 25%, the nearest neighbour weighting is 0.5 and the critical size is 100.

3.4. Kinetic analysis

The time-dependence of the fractional conversion, α, of anatase to rutile predicted by the simulation has been compared [16] with the widely used relationship, Eq. (1), i.e. $\alpha = 1 - \exp(-kt^n)$.

This may be rearranged to the form

$$\log(-\ln(1-\alpha)) = \log k + n\ \log(t) \tag{10}$$

If MCS, the number of Monte Carlo steps, is substituted for the time, t, a linear plot of $\log(-\ln(1-\alpha))$ versus log(MCS) is expected if the simulated transformation conforms to Eq. (1). Fig. 6 shows the results of this analysis for $k_BT/J = 1$, $f = 0.25$, $\omega_s/\omega_f = 0.5$ and $20 < S_L < 120$. Although none of the plots is

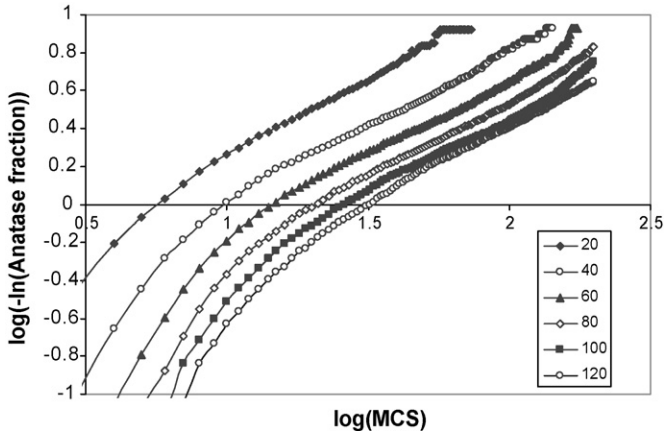

Fig. 6. Plot of log(−ln(anatase fraction)) versus log(MCS) for selected values of critical size S_L. The occupancy is 25%, the nearest neighbour weighting is 0.5 and the temperature parameter is 1.0.

linear, because of the common induction effect, for every S_L value there is a range of MCS over which the linear relationship holds and the goodness of fit may be conveniently represented by the R^2 values (where R is the familiar Pearson product moment coefficient). Over a log(MCS) range of 0.5, the MCS values for maximum R^2 (>0.999 in all cases) were first determined by inspection, and the slopes, n, and intercepts, k, of these lines were then tabulated. Table 2 summarizes these results both for the best fit lines and, so that the sensitivity to the selection of MCS range can be assessed, for selected non-optimal comparisons. The tabulation demonstrates that for all values of S_L, there is a region of the transformation plot in which Eq. (10) is obeyed. This region occurs at increasing numbers of Monte Carlo steps as S_L increases, a natural consequence of the greater time needed for anatase to grow to the specified larger critical size. In all cases $n = 0.73 \pm 0.03$ and the tabulation confirms the visual impression that although a rather moderate range (log(MCS) = 0.5) has been selected for this analysis the transformation curves remain approximately parallel over a wider range of simulation times. The value of n is significantly lower than the generally accepted values of $n = 2$ for site-saturation nucleation, or $n = 3$ for continuous nucleation during the transformation of a continuous phase.[23] However, Shlesinger and Montroll[24] have demonstrated that $0 < n < 1$ for defects hopping in a random environment with a hierarchy of waiting times and Klafter and Shlesinger[25] have demonstrated that a number of different physical models lead in a natural way to values of $n = 0.5$ for 1 dimension and $n = 1$ for 3 dimensions. A kinetic Ising model for polymer dynamics[26] led to values between 0.5 and 0.74. Our current value of $n = 0.73$ for this 2-dimensional simulation does not seem unreasonable.

An analysis at fixed S_L, for $k_B T/J$ varying between 1 and 5 leads to a similar pattern of results although the spread of the transformation curves is smaller. It is of interest to note that the transformation curve corresponding to $k_B T/J = 0.67$ (the values at which the growth curve showed a discontinuity) was unexceptional.

Table 2
The range of MCS, over which α, the fractional conversion to rutile, is satisfactorily represented by the equation $\alpha = 1 - \exp(-kt^n)$ where t = the number of MCS and k and n are constants with values shown in the Table

	Range of log (MCS) 1.00–1.50	Range of log (MCS) 1.20–1.70	Range of log (MCS) 1.30–1.80	Range of log (MCS) 1.40–1.90	Range of log (MCS) 1.45–1.95	Range of log (MCS) 1.55–2.05	Range of log (MCS) 1.65–2.15
$S_L = 20$	$n = 0.76 \pm 0.04$, $k = -0.5_3$, $R^2 = 0.99_9$	$n = 0.83 \pm 0.04$, $k = -0.5_8$, $R^2 = 0.99_5$		$n = 0.85 \pm 0.04$, $k = -0.6_1$, $R^2 = 0.97_7$			
$S_L = 40$		$n = 0.70 \pm 0.04$, $k = -0.6_4$, $R^2 = 0.99_9$		$n = 0.75 \pm 0.04$, $k = -0.7_2$, $R^2 = 0.99_8$			
$S_L = 60$			$n = 0.70 \pm 0.04$, $k = -0.7_7$, $R^2 = 0.99_9$	$n = 0.70 \pm 0.04$, $k = -0.7_7$, $R^2 = 0.99_9$			
$S_L = 80$				$n = 0.74 \pm 0.04$, $k = -0.9_5$, $R^2 = 0.99_9$	$n = 0.73 \pm 0.04$, $k = -0.9_4$, $R^2 = 0.99_9$		
$S_L = 100$				$n = 0.75 \pm 0.04$, $k = -1.04_2$, $R^2 = 0.99_6$	$n = 0.71 \pm 0.04$, $k = -0.9_9$, $R^2 = 0.99_6$	$n = 0.69 \pm 0.04$, $k = -0.9_4$, $R^2 = 0.99_9$	
$S_L = 120$				$n = 0.85 \pm 0.04$, $k = -1.2_7$, $R^2 = 0.99_4$			$n = 0.74 \pm 0.04$, $k = -1.1_6$, $R^2 = 0.99_9$

The 'goodness of fit' is represented by the value of R^2.

3.5. Spread of crystal sizes

As the simulation progresses, anatase crystals are progressively replaced by rutile crystals. Rutile has a higher refractive index than anatase and therefore scatters light more efficiently; i.e., rutile is the better opacifying pigment. For pigmentary applications of TiO_2 a narrow spread of crystal sizes is desirable because light-scattering is also sensitive to the ratio of crystal size, d, to wavelength, λ. More efficient scattering results if the crystal sizes are clustered more closely around the optimum value of d/λ. Therefore, both the standard deviation of the size and the corresponding normalized deviation, (obtained by dividing the standard deviation by the mean size) of the rutile crystals formed by the transformation have been calculated for different values of the critical size, Fig. 8, and for different values of the temperature parameter, Fig. 7.

Fig. 7a shows the almost linear dependence of the root mean square deviation of the rutile crystal-size on MCS. The spread of sizes increases as the temperature parameter increases from 0 to 1 and then decreases as k_BT/J increases from 1 to 2. At $k_BT/J = 0.67$, the value at which the size for fixed composition shows a discontinuity (Fig. 5), the behaviour is unexceptional. Although the size-spread increases with increasing MCS, the rutile size also increases (Fig. 4b) so that the normalized deviation, rms/⟨R⟩, is relatively constant for increasing MCS (Fig. 7b). The effect of k_BT/J on rms/⟨R⟩ is very small in the range 0–0.67 but increases significantly from 0.67 to 2.0. This is consistent with the previously described insensitivity of mean size with k_BT/J values below 0.67 and the subsequent fall in mean size at larger k_BT/J. The pattern of rms/⟨R⟩ is controlled by the behaviour of ⟨R⟩.

For $k_BT/J \leq 1$, plots of normalized deviation versus mean rutile size (Fig. 7c) show minima. For $k_BT/J = 0.5$ the minimum is at a rutile fraction of 0.50, whereas for $k_BT/J = 1$ the minimum is at a rutile fraction of 0.76 although both curves have a minimum close to ⟨R⟩ ≈ 270. Fig. 7d suggests that the normalized deviation increases by a small amount as the fraction of rutile increases from 0.75 to ca. 0.98, typical of sulphate-route[2] rutile pigments. There is, once more, increasing dependence on the temperature parameter when $k_BT/J \geq 0.67$.

Fig. 8 summarizes the corresponding analysis of the dependence of rutile size-distribution on the choice of critical size, S_L. In Fig. 8a the almost linear dependence of the root mean square (rms) deviation of the rutile crystal size on MCS is much less affected by changes in S_L (from 20 to 120) than by changes in the temperature parameter (Fig. 7a). Most curves converged by 200 MCS, probably because the mean size, ≥400, significantly exceeded the largest critical size ($S_L = 120$) and hence

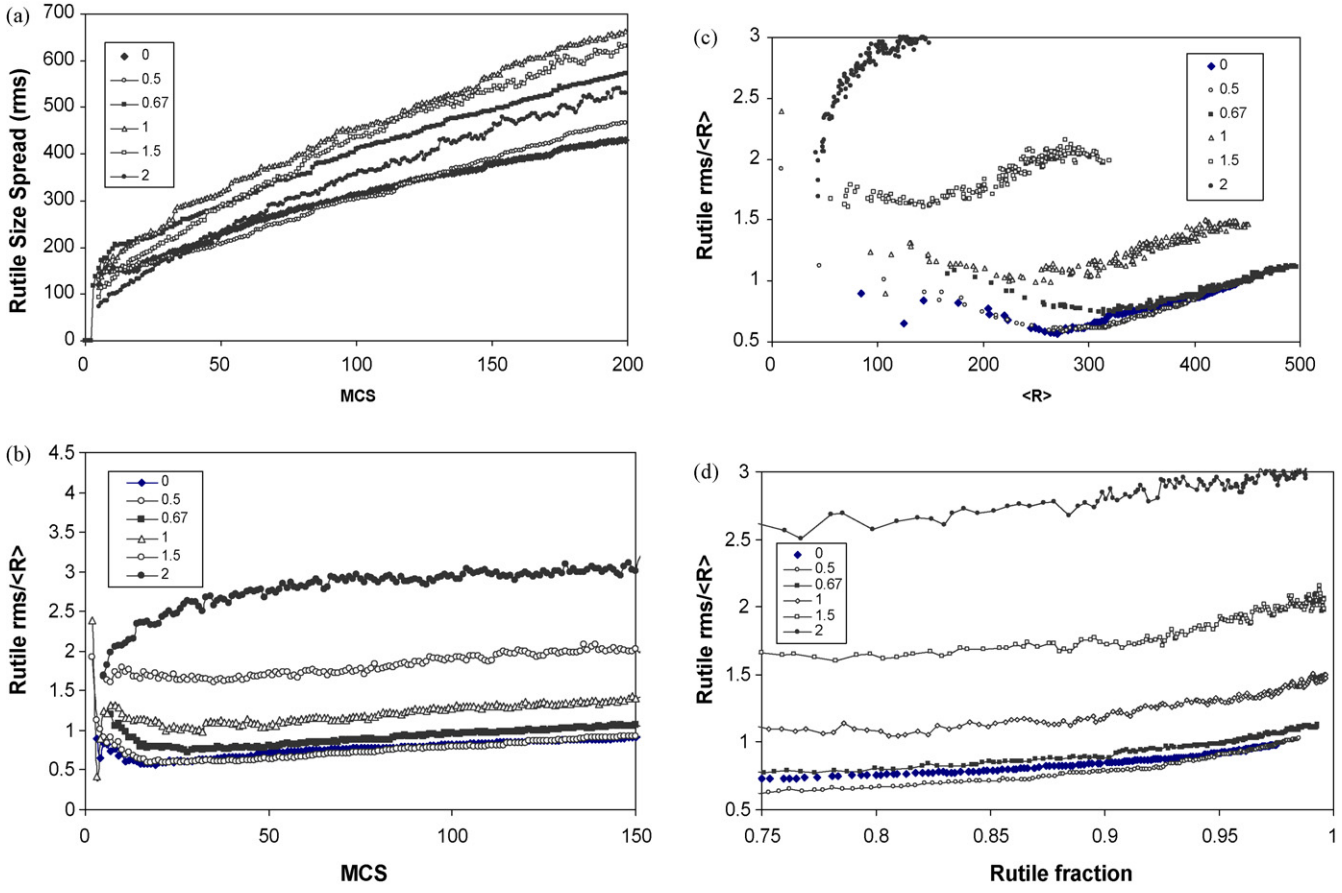

Fig. 7. For selected values of temperature parameter (k_BT/J), (a) rutile size-spread (rms) versus MCS. (b) Normalized rutile rms (rms/⟨R⟩) versus MCS. (c) Normalized rutile rms (rms/⟨R⟩) versus rutile mean size (⟨R⟩). (d) Normalized rutile rms (rms/⟨R⟩) versus rutile fraction. In all cases, the occupancy is 25%, the nearest neighbour weighting is 0.5 and the critical size is 100.

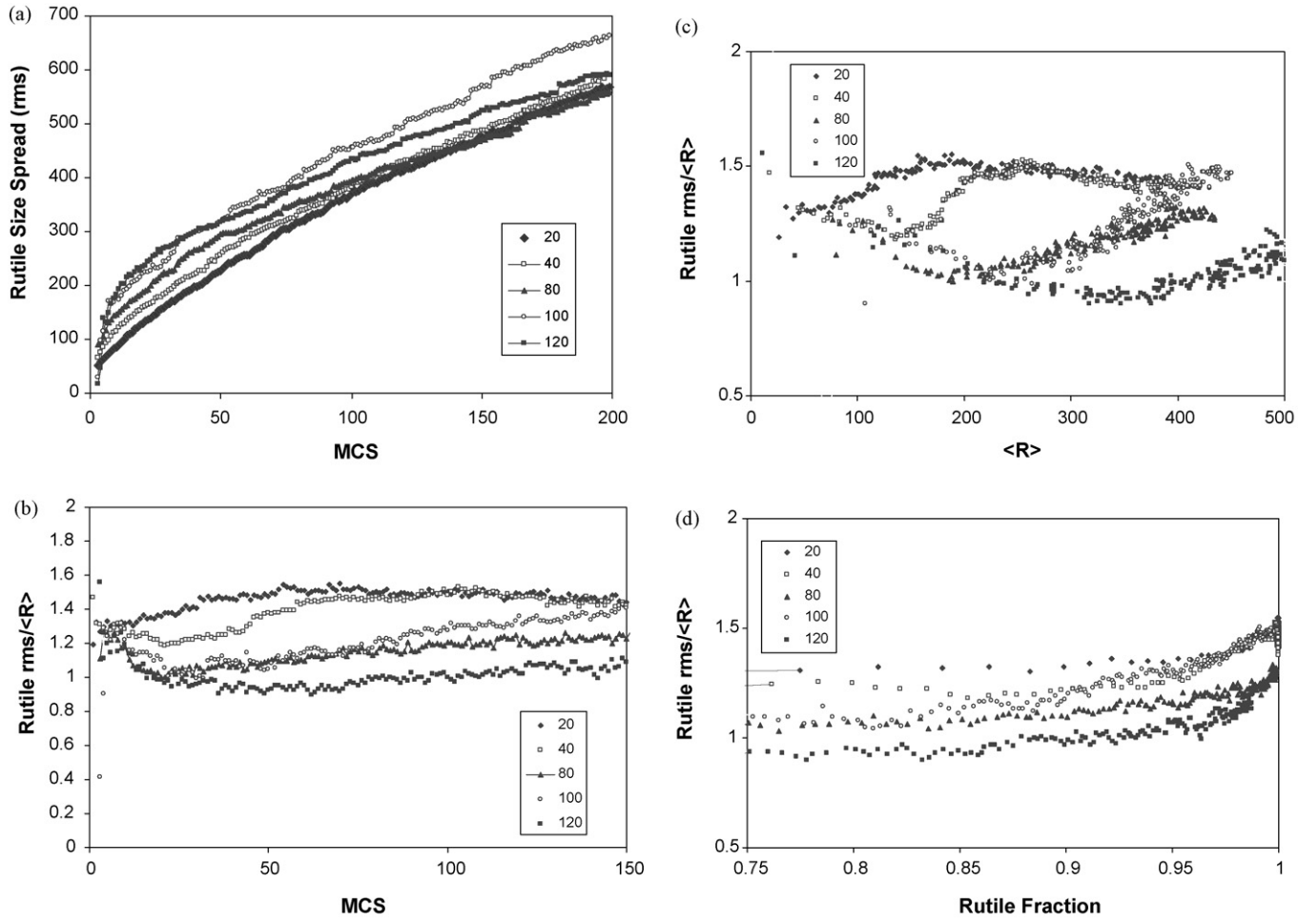

Fig. 8. For selected values of critical size (S_L), (a) rutile size-spread (rms) versus MCS. (b) Normalized rutile rms (rms/⟨R⟩) versus MCS. (c) Normalized rutile rms (rms/⟨R⟩) versus rutile mean size (⟨R⟩). (d) Normalized rutile rms (rms/⟨R⟩) versus rutile fraction. In all cases, the occupancy is 25%, the nearest neighbour weighting is 0.5 and the temperature parameter is 1.0.

the 'memory' of differences in S_L no longer dominated. The corresponding normalized deviations, Fig. 8b, showed a monotonic decrease in rms/⟨R⟩ as S_L increased, a consequence of the increase in ⟨R⟩ with increasing S_L (Fig. 3b) as discussed earlier. Again the results were less sensitive to changes in S_L than to variation in k_BT/J. In Fig. 8c, plots of rms/⟨R⟩ versus the mean rutile size ⟨R⟩ show minima (except for $S_L = 20$) which are less pronounced than in the corresponding plots, Fig. 7c, in which the temperature parameter was varied. For $k_BT/J = 1$, the common temperature parameter for Fig. 8, the smallest values of the normalized size-spread were obtained for large values of S_L; a similar but much smaller effect was obtained for $k_BT/J = 2$ (not shown). The most significant aspect of the plots of rms/⟨R⟩ versus rutile fraction, Fig. 8d, is the absence of minima. The normalized deviations gradually increase as the rutile fraction increases from 0.75 to 0.98. These increases are less than the change from ∼1 to ∼1.3 as S_L decreases from 120 to 20, at a fixed rutile fraction of 0.98. Minima were also absent from the results of simulations with $k_BT/J = 2$ (not shown) even though the absolute values of the normalized spread were larger. At these higher values of the temperature parameter the normalized spread increased as S_L increased.

4. Concluding remarks

The simulations have shown that estimates of the amount of rutile formed, %R, and of the mean sizes of anatase and rutile, ⟨A⟩ and ⟨R⟩, respectively, obtained by averaging five Monte Carlo simulations have satisfactory repeatability and allow the effect of the different model parameters to be evaluated. As in an earlier study, of crystal growth without the possibility of transformation to rutile, crystal growth was influenced by the temperature parameter k_BT/J, which controls the probability of accepting an individual evaporation condensation step. At $k_BT/J \approx 0.67$ a discontinuity occurred in a plot of mean size, at fixed composition, against temperature parameter.

There was an induction period for transformation of anatase to rutile which increased with increasing S_L and which limited the applicability of a simple analytical representation of the transformation kinetics. However, for every S_L, there was a range over which the simulation results were satisfactorily represented by the familiar relation $\alpha = 1 - \exp(-kt^n)$, with $n \approx 0.75$.

Increases in S_L, the minimum size at which anatase could convert to rutile, increase both the anatase mean size (and $\langle A \rangle \approx 0.5 S_L$) and the rutile mean size, ⟨R⟩ corresponding to a

fixed number of MCS. Very large increases of $\langle R \rangle$ during the last stages of the anatase to rutile conversion suggest that practical attempts to exceed 98% conversion during calcination would lead to a large range of crystal sizes. In general, the normalized crystal-size distributions, $\delta/\langle R \rangle$, predicted by the model are much less affected by changes in S_L than by differences in $k_B T/J$. For rutile the normalized size distribution, $\delta/\langle R \rangle$, increased smoothly as the rutile fraction increased from 0.75 to 0.98.

Acknowledgements

This work was initiated within the ACORN programme of the IMPACT Faraday Partnership supported by the UK Dept. of Trade & Industry and EPSRC. We thank, the then, Huntsman Pigments for its sponsorship and Mr. Mike Westwood and Dr. John Edwards of Huntsman Pigments for many helpful discussions.

References

1. Egerton, T. A., (*4th ed.*). *Titanium Compounds in Kirk Othmer Encyclopedia of Chemical Technology*, *vol. 24*John Wiley & Sons, New York, 1997, pp. 226–274.
2. Egerton, T. A. and Tetlow, A., Titanium Dioxide Products in *Industrial Inorganic Chemicals*, In R. Thompson, ed. Royal Society of Chemistry, Cambridge, UK, pp. 351–372.
3. JANAF Thermochemical Tables (3rd ed.). *J. Phys. Chem. Ref. Data*, 1985, **14**(Supplement 1).
4. Amores, J. M. G., Escribano, V. S. and Busca, G., Anatase crystal growth and phase transformation to rutile in high area TiO_2, MoO_3-TiO_2, and other TiO_2-supported oxide catalytic systems. *J. Mater. Chem.*, 1995, **5**, 1245–1249.
5. Ranade, M. R., Navrotsky, A., Zhang, H. Z. *et al.*, Energetics of nanocrystalline TiO_2. *Proc. Nat. Acad. Sci.*, 2002, **99**(April (Suppl. 2)), 6476–6481.
6. Navrotsky, A., Calorimetry of nanoparticles, surfaces, thin films and multilayers. *J. Chem. Thermodynamics*, 2007, **39**, 2–9.
7. Mitsuhashi, T. and Kleppa, O. J., Transformation enthalpies of the TiO_2 polymorphs. *J. Am. Ceram. Soc.*, 1979, **62**, 356–357.
8. Zhang, H. Z. and Banfield, J. F., Thermodynamic analysis of phase stability of nanocrystalline titania. *J. Mater. Chem.*, 1998, **8**, 2073–2076.
9. Zhang, A. H. and Banfield, J. F., Kinetics of crystallization and crystal growth of nanocrystalline anatase in nanometer-sized amorphous titania. *Chem. Mater.*, 2002, **14**, 4145–4154.
10. Finnegan, M. P., Zhang, H. and Banfield, J. F., Phase transformation and stability in titania particles in aqueous solutions dominated by surface energy. *J. Phys. Chem.*, 2007, **111C**, 1962–1968.
11. Gribb, A. A. and Banfield, J. F., Particle size effects on transformation kinetics and phase stability in nanocrystalline TiO_2. *J. Am. Miner.*, 1997, **82**, 717–728.
12. Zhang, H. Z. and Banfield, J. F., Understanding polymorphic phase transformation behavior during growth of nanocrystalline aggregates, insight from TiO_2. *J. Phys. Chem.*, 2000, **104B**, 3481–3487.
13. Shannon, R. D. and Pask, J. A., Kinetics of the anatase-rutile transformation. *J. Am. Ceram. Soc.*, 1968, **48**, 391–398.
14. Okada, K., Yamamoto, N., Kameshima, Y., Yasumori, A. and Mackenzie, K. J. D., Effect of silica additive on the anatase-to-rutile phase transition. *J. Am. Ceram. Soc.*, 2001, **4**, 1591–1596.
15. Madras, G., McCoy, B. J. and Navrotsky, A., Kinetic model for TiO_2 polymorphic transformation from anatase to rutile. *J. Am. Ceram. Soc.*, 2007, **90**, 250–255.
16. Zhang, H. and Banfield, J. F., Phase transformation of nanocrystalline anatase-to-rutile via combined interface and surface nucleation. *J. Mater. Res.*, 2000, **15**, 437–448.
17. Zhang, H. and Banfield, J. F., Kinetics of crystallization and crystal growth of nanocrystalline anatase in nanometer-sized amorphous titania. *Chem. Mater.*, 2002, **14**, 4145–4154.
18. Qiu, F., Egerton, T. A. and Cooper, I. L., An extended two-state model for grain growth during gas-phase production of powders. *J. Eur. Ceram. Soc.*, 2006, **26**, 37–47.
19. Binder, K. and Heerman, D. W., *Monte Carlo Simulation in Statistical Physics* (*4th ed.*). Springer, Berlin, 2002.
20. Madras, G. and McCoy, B. J., Ostwald ripening with size dependent rates: similarity and power-lay solutions. *J. Chem. Phys.*, 2002, **117**, 8042–8049.
21. Madras, G. and McCoy, B. J., Ostwald ripening in two dimensions: time dependence of size distributions for thin film islands. *Phys. Chem. Chem. Phys.*, 2003, **5**, 5459–5466.
22. Zhang, H. and Banfield, J. F., Size dependence of the kinetic rate constant for phase transformation in TiO_2 nanoparticles. *Chem. Mater.*, 2005, **17**, 3421–3425.
23. Iwamatsu, M. and Nakamura, M., Cell dynamics simulation of Kolmogorov-Johnson-Mehl-Avrami kinetics of phase transformation: one and two-dimensional cases. *Mater. Sci. Eng.*, 2007, **A449–451**, 671–674.
24. Shlesinger, M. F. and Montroll, E. W., On the Williams-Watts function of dielectric-relaxation. *Proc. Natl. Acad. Sci. U.S.A.*, 1984, **81**, 1280–1283.
25. Klafter, J. and Shlesinger, M. F., On the relationship among 3 theories of relaxation in disordered-systems. *Proc. Natl. Acad. Sci. U.S.A.*, 1986, **83**, 848–851.
26. Skinner, J. L., Kinetic ising-model for polymer dynamics—applications to dielectric-relaxation and dynamic depolarized light-scattering. *J. Chem. Phys.*, 1983, **79**, 1955–1964.